

# HARMONIC GENERATION IN TWO ORTHOGONAL UNDULATORS\*

Najmeh Sadat Mirian<sup>†</sup>

UVSOR Facility, Institute for Molecular Science (IMS), Okazaki, Japan and  
School of Particle and Accelerator Physics, IPM, Tehran, Iran

## Abstract

In this report, the harmonic generation in two orthogonal undulators is under discussion. There is a possibility of generation of the even and odd harmonics as well as non-integer harmonics in two orthogonal undulators. By considering the first order of electron velocity, the total energy radiated per unit solid angle per unit frequency interval for a single electron traveling along the undulators is derived. Also a numerical simulation of one-dimensional non-averaged equations is conducted to present the self amplified spontaneous emission of harmonic generation in two orthogonal undulators.

## INTRODUCTION

Modern high intensity sources are based on the electron radiation through undulator in synchrotrons and free electron lasers (FEL). Free electron lasers that are mostly based on self amplified spontaneous emission, hold great prospects as high power, coherent, and tunable radiation in the high frequency region of the electromagnetic spectrum [1,2]. The angular distribution of the radiation in undulators is obtained by computing the amount of energy lost by the particle in a retarded time during the emission of the signal. In practice, the spectrum of the radiation depends on the detailed motion of the electron and on the direction from which the electron is observed.

In a planar undulator with an ideal sinusoidal periodic magnetic field, the electrons radiate at odd harmonics due to their non-uniform axial motion. In ideal helical undulator, because of the constant longitudinal velocity, the spectrum is centered about the resonance frequency and there is no significant harmonic growth.

The two orthogonal undulators in FEL has been proposed as away toward the product of two tunable color radiation pulses with different polarizations, while the total length of device dose not change with the respect to the usual single-color FEL [3,4]. The form of this undulator is composed of two linear undulators orthogonally polarized with different periods. The possibility of generation of two radiation waves with different frequencies and different polarizations was investigated. We showed that by changing dependently the strength of the two magnetic fields, we can control the final power and the saturation length.

This report focuses on studying the harmonic generation in the two-orthogonal undulators in two different methods.

\* Work supported by Institute for Research in Fundamental Sciences (IPM)  
<sup>†</sup> nsmirian@ims.ac.jp

## FIELD EQUATIONS

The undulator magnetic field, in the paraxial approximation, is described by the following expression

$$\mathbf{B}_w = B_{w2} \cos(k_{02}z) \hat{e}_x + B_{w1} \cos(k_{01}z) \hat{e}_y, \quad (1)$$

where  $B_{wi}$  is the untapered undulator field amplitude,  $k_{01,02} = 2\pi/\lambda_{01,02}$  are undulator wave numbers and  $K_{1,2} = |eB_{w1,2}\lambda_{01,2}/mc^2|$  are the deflecting parameters. We assume  $n\lambda_{01} = m\lambda_{02}$ , which permits us to treat the cases of a harmonic relation between  $\lambda_{01}$  and  $\lambda_{02}$  and of rational  $m/n$ . The proper resonance relation in this magnetic file has been obtained as [3,4]

$$\lambda_{1,2} = \frac{\lambda_{01,02}}{\gamma} \left( 1 + \frac{K_1^2}{2} + \frac{K_2^2}{2} \right), \quad (2)$$

where  $\lambda_1$  and  $\lambda_2$  are, respectively, fundamental resonance wavelength in the x and y direction. The one-dimensional vector potential can be assumed to be

$$\mathbf{A} = i \sum_h \left[ A_{1h} e^{i(k_{1z}z - \omega_1 t)} \hat{e}_x + A_{2h} e^{i(k_{2z}z - \omega_2 t)} \hat{e}_y \right], \quad (3)$$

where  $h$  is the harmonic number. The vector potential amplitudes  $A_{1,2h} = A_{1,2h}^{(1)} + i A_{1,2h}^{(2)}$ , are assumed to vary slowly in  $z$  and  $t$ . By using Maxwell-Poisson equation in Gaussian gauge, and the slowly varying envelope approximation (SVEA), the two polarization amplitudes take the following independent differential form:

$$\frac{\partial}{\partial z} A_{1,2h} + \frac{1}{c} \frac{\partial}{\partial t} A_{1,2h} = \frac{2\pi en}{k_{1,2}} \sum_h \beta_{x,y} \delta(z - z_j) e^{-i\alpha_{1,2h}j}, \quad (4)$$

$$\alpha_{1,2h} = h(k_{1,2}z - \omega_{1,2}t) = h\alpha_{1,2},$$

where  $\omega_{1,2} = k_{1,2}c$  is radiation frequency for fundamental resonance. Similar to the way used in Ref [4] after averaging of Maxwell's equation over time scale  $\ell/c$  (where  $\ell = n\lambda_1 = m\lambda_2$ ), we have

$$\left( \frac{\partial}{\partial z} - \frac{\partial}{\partial t} \right) \begin{pmatrix} a_{1h}^{(1)} \\ a_{1h}^{(2)} \end{pmatrix} = \frac{\omega_p^2}{2h\omega_1 c} \beta_{z,0} \begin{pmatrix} \left\langle \frac{u_x}{|u_z|} \cos(\alpha_{1h}) \right\rangle \\ - \left\langle \frac{u_x}{|u_z|} \sin(\alpha_{1h}) \right\rangle \end{pmatrix}, \quad (5)$$

$$\left( \frac{\partial}{\partial z} - \frac{\partial}{\partial t} \right) \begin{pmatrix} a_{2h}^{(1)} \\ a_{2h}^{(2)} \end{pmatrix} = \frac{\omega_p^2}{2h\omega_1 c} \beta_{z,0} \begin{pmatrix} \left\langle \frac{u_y}{|u_z|} \cos(\alpha_{2h}) \right\rangle \\ - \left\langle \frac{u_y}{|u_z|} \sin(\alpha_{2h}) \right\rangle \end{pmatrix}, \quad (6)$$

$a_h^{(1,2)} = e \frac{A_h^{(1,2)}}{mc^2}$  is the normalized amplitude,  $\omega_p^2 = 4\pi e^2 n/mc^2$  is the square of plasma frequency, and  $\mathbf{u} = \mathbf{P}/mc = \gamma\beta$  is a dimensionless variable. The averaging operator is defined as

$$\langle(\dots)\rangle = \int_0^{2\pi} \frac{\sigma(\psi_0)}{2\pi} d\psi_0(\dots), \quad (7)$$

where  $\sigma(\psi_0)$  is the phase distribution at the entry time  $t_0$ , and  $\psi_0$  is the initial phase  $\psi_0 = \omega t_0$ .

## MOMENTUM EQUATION

By using Lorentz force equation, the momentum equations for the  $i$ th electron of the beam can be derived as

$$\begin{aligned} \frac{dp_{ix,y}}{dt} &= e\beta_{iz}B_{w1,2} \cos(k_{01,2}z) \\ &\quad - \sum_h ehk_{1,2}(1 - \beta_{iz})[A_{1,2h}e^{ih\alpha_{i1,2}} + cc], \\ \frac{dp_{iz}}{dt} &= e\beta_{iy}B_{w2} \cos(k_{02}z) - \sum_h ehk_2\beta_{iy}[A_{2h}e^{ih\alpha_{i2}} + cc] \\ &\quad - eh\beta_{ix}B_{w1} \cos(k_{01}z) - \sum_h ek_1\beta_{ix}[A_{1h}e^{ih\alpha_{i1}} + cc], \end{aligned} \quad (8)$$

where  $\beta_{x,y,zj} = v_{x,y,zj}/c$  are the normalized velocity components. In first order longitudinal velocity takes following form [4]

$$\beta_z = \frac{1}{4} \left[ \left( \frac{K_1}{\gamma} \right)^2 \cos(2k_{01}z) + \left( \frac{K_2}{\gamma} \right)^2 \cos(2k_{02}z) \right] + \beta_0, \quad (9)$$

where  $\beta_0^2 = 1 - 1/\gamma^2$ . The trajectories of the electrons in first order takes form:

$$\begin{aligned} \mathbf{r}_j &= \beta_0 ct \hat{e}_z - \frac{\lambda_{01}}{2\pi} \frac{K_1}{\gamma_0} \sin(\omega_{01}t) \hat{e}_x - \frac{\lambda_{02}}{2\pi} \frac{K_2}{\gamma_0} \sin(\omega_{02}t) \hat{e}_y \\ &+ \frac{\lambda_{01}}{16\pi} \left( \frac{K_1}{\gamma_0} \right)^2 \sin(2\omega_{01}t) \hat{e}_z + \frac{\lambda_{02}}{16\pi} \left( \frac{K_2}{\gamma_0} \right)^2 \sin(2\omega_{02}t) \hat{e}_z. \end{aligned} \quad (10)$$

$$\begin{aligned} \frac{d^2I}{d\omega d\Omega} &= \frac{e^2}{\gamma^2 \omega_{01}^2 c} \left\{ \left[ K_1 \sum_d \sum_{d'} J_d(\chi_1) J_{d'}(\chi_2) \left( \frac{\sin\left(\frac{(\omega - \omega_r(1-2(d-d'\zeta))N\pi)}{\omega_r}\right)}{\left(\frac{(\omega - \omega_r(1-2d-d'\zeta))N\pi}{\omega_r}\right)}\right) - \frac{\sin\left(\frac{(\omega - \omega_r(1+2(d+d'\zeta))N\pi)}{\omega_r}\right)}{\left(\frac{(\omega - \omega_r(1+2(d+d'\zeta))N\pi)}{\omega_r}\right)} \right] \right]^2 + \right. \\ &\quad \left. \left[ K_2 \sum_d \sum_{d'} J_d(\chi_1) J_{d'}(\chi_2) \left( \frac{\sin\left(\frac{(\omega - \omega_r(\zeta-2(d+d'\zeta))N\pi)}{\omega_r}\right)}{\left(\frac{(\omega - \omega_r(\zeta-2(d+d'\zeta))N\pi)}{\omega_r}\right)}\right) - \frac{\sin\left(\frac{(\omega - \omega_r(\zeta+2(d+d'\zeta))N\pi)}{\omega_r}\right)}{\left(\frac{(\omega - \omega_r(\zeta+2(d+d'\zeta))N\pi)}{\omega_r}\right)} \right] \right]^2, \end{aligned} \quad (15)$$

Equation (15) shows depending on value of  $\zeta$ , we can have even and odd harmonics. If  $\zeta$  is the odd number, instead, odd harmonics domain. As well, if  $\zeta$  is even, certainly we have growth of even harmonics. Further, this equation shows in some cases we can observe the no-integer harmonics.

Figure 1 displays this equation for different values of  $\zeta$  at  $z=4$  m. As can be seen in case (c) where the  $\zeta$  is non-integer number, we can observe the integer and non-integer harmonics.

## HARMONIC GENERATION

The total energy radiated per unit solid angle per unit frequency interval for a single electron in an undulator with length  $L_w = N_w \lambda_{0i}$  is obtained by

$$\frac{d^2I}{d\omega d\Omega} = \frac{e^2}{4\pi^2 c} \left| \int_{-L_w/2c}^{L_w/2c} dt \mathbf{n} \times [\mathbf{n} \times \boldsymbol{\beta}(t)] e^{i\omega[t - \mathbf{n} \cdot \mathbf{r}(t)/c]} \right|^2, \quad (11)$$

here,  $\mathbf{n}$  is a unit vector from the electron to the observer. Only the emission in the forward direction ( $\mathbf{n} = \hat{e}_z$ ) is considered, then

$$\begin{aligned} \hat{e}_z \cdot \mathbf{r} &\approx \beta_0 ct + \frac{\lambda_{01}}{16\pi} \left( \frac{K_1}{\gamma_0} \right)^2 \sin(2\omega_{01}t) + \frac{\lambda_{02}}{16\pi} \left( \frac{K_2}{\gamma_0} \right)^2 \\ &\quad \times \sin(2\omega_{02}t), \end{aligned} \quad (12)$$

$\hat{e}_z \times [\hat{e}_z \times \boldsymbol{\beta}(t)] = -\frac{1}{\gamma} [K_1 \sin(\omega_{01}t) + K_2 \sin(\omega_{02}t)]$ , where  $\omega_{01,2} = k_{01,2}c$ . By using following expansion

$$e^{-i\xi \sin\theta} = 2\pi \sum_{l=-\infty}^{l=\infty} J_l(\xi) e^{-il\theta}, \quad (13)$$

where  $J_l(\zeta)$  is a Bessel function of the first kind, one can write

$$\begin{aligned} \hat{e}_z \times [\hat{e}_z \times \boldsymbol{\beta}(t)] e^{i\omega(t - \hat{e}_z \cdot \mathbf{r}/c)} &= \frac{2\pi}{2i\gamma^2} \sum_d \sum_{d'} [J_d(\chi_1) J_{d'}(\chi_2) \\ &K_1 [e^{it(\omega(1-\beta_0) - \omega_0(2(d+d'\zeta)-1))} - e^{it(\omega(1-\beta_0) - \omega_0(2(d+d'\zeta)+1))}] \hat{e}_x \\ &+ K_2 [e^{it(\omega(1-\beta_0) - \omega_0(2(d+d'\zeta)-\zeta))} - e^{it(\omega(1-\beta_0) - \omega_0(2(d+d'\zeta)+\zeta))}] \hat{e}_y], \end{aligned} \quad (14)$$

here,  $\chi_{1,2} = K_{1,2}\omega/8\pi c\gamma^2 k_{w1,2}$ , and  $\zeta = \omega_2/\omega_1 = m/n$ . Therefore, by integration of Eq. (14) in Eq.(11), we have

Polarization angle of radiation is another important issue in two orthogonal undulators. However, we know it depends on the magnetic field intensity of each undulator. Figure 2 presents the radiation polarization angle in various frequencies.

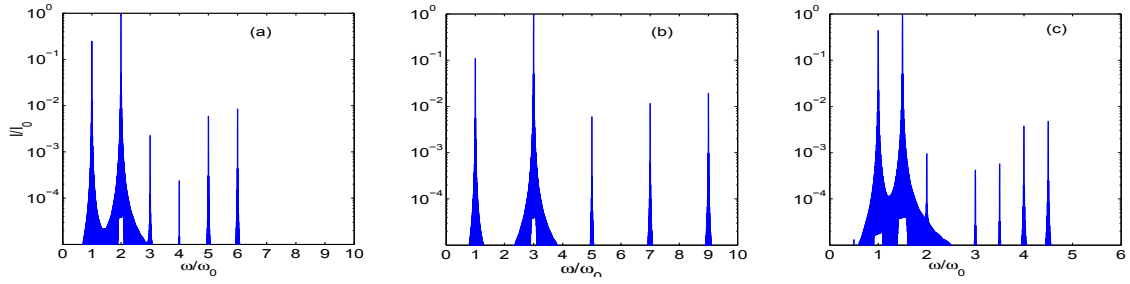


Figure 1: Spectrum of the radiation of one electron at  $z=4$  m (a)  $m/n=2$ , (b)  $m/n=3$  and (c)  $m/n=3/2$ ,  $K_1 = K_2 = 2.1$ ,  $\lambda_{01} = 2.8$  cm.

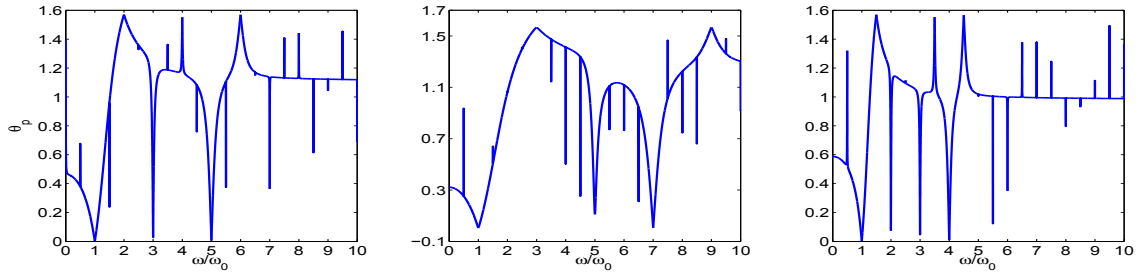


Figure 2: Radiation polarization angle of one electron radiation, while (a)  $m/n=2$ , (b)  $m/n=3$  and (c)  $m/n=3/2$ ,  $K_1 = K_2 = 2.1$ ,  $\lambda_{01} = 2.8$  cm.

## TIME DEPENDENT SIMULATION AND SHOT NOISE ALGORITHM

The set of the vector potential fields, phases and the non averaged dynamic equations includes  $4N_e + 2N_h$  self-constant first order differential equations, where  $N_e$  indicates the macroparticle numbers in one beamlet, and  $N_h$  is the number of harmonics. In this case the length of the beamlet is  $\ell = n\lambda_1 = m\lambda_2$ . For simulation, we extended the Cyrus 1D code [6]. Cyrus 1D follows the approach of MEDUSA 1D [5]. This code shows very significant agreement with T1 code [7] corresponding to averaged FEL code and logistic map formula proposed with G. Dattoli [8].

To include shot noise in the simulation, the macroparticles are assumed to load over  $[0, 2\pi]$  and perturbation due to shot noise is imposed to the phases, such that

$$\alpha'_j = \alpha_j + \delta\alpha \sin(\alpha_j - \phi)$$

where  $\phi$  is chosen randomly over the interval  $[0, 2\pi]$  and  $\delta\alpha \ll 1$  describe the Poisson statistics. The phase of macroparticle, in x-polarization and y-polarization of electromagnetic radiation, are defined as

$$\alpha_{1j} = n\alpha'_j, \quad \alpha_{2j} = m\alpha'_j. \quad (16)$$

For time dependent (i.e slippage) simulation we use approach explained in Ref [9], however in this case the electron bunch with  $L_b$  length is divided to  $L_b/\ell$  slices and the time de-

pendent operation in Rung-Kutta loop is imposed on every spatial interval  $\ell_w = n\lambda_1 = m\lambda_2$ .

In simulation the electron current is assumed to be 100 A and  $\gamma = 300$ . Fig.3 presents the evolution of pulse energy of (a) x-polarization ( $\lambda_1$ ) and (b) y-polarization ( $\lambda_2$ ) for different harmonics through undulator interaction, while the  $m/n = 2/1$ . It shows the growth of the even harmonics as well as the odd harmonics. For x-polarization, the intensity of the fifth harmonic at saturation point is higher than intensity of the third harmonic. For y-polarization, the intensity of the second harmonic is higher than the odd harmonics.

Figure 4 shows, when  $m/n=3/1$ , both  $m$  and  $n$  are the odd number, the odd harmonics of the x-polarization and y-polarization have higher intensity respect to the even harmonics. In fact, the growth of the odd harmonics are faster. Further, this plot shows that the pulse energy at the saturation point,  $z=4$  m, for the third harmonic of the x-polarization, which has the wavelength equal to the fundamental resonance of the y-polarization, is higher than the fundamental resonance of x-polarization.

Figure 5 demonstrates the evolution of harmonic pulse energy, when  $m/n=3/2$ . Plat (a) indicates that the energy of the second harmonic pulse is equal to the third harmonic pulse energy at  $z=6$  m.

Figures 6 and 7 show the pulse shape near saturation point  $z = 4.5$  m, for different harmonics of x-polarization and y-polarization when, respectively,  $m/n = 2$  and  $m/n = 3$ .

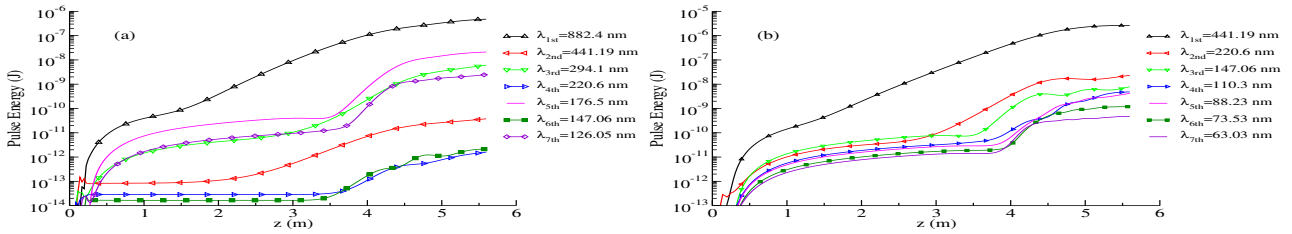


Figure 3: Evolution of pulse energy through undulator interaction for different harmonics (a) x- polarization , (b) y- polarization,  $m/n=2/1$ .

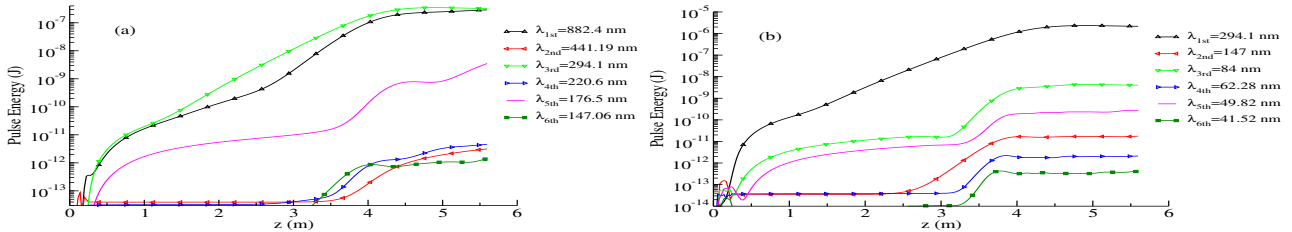


Figure 4: Evolution of pulse energy through undulator interaction for different harmonics (a) x- polarization , (b) y- polarization,  $m/n=3/1$ .

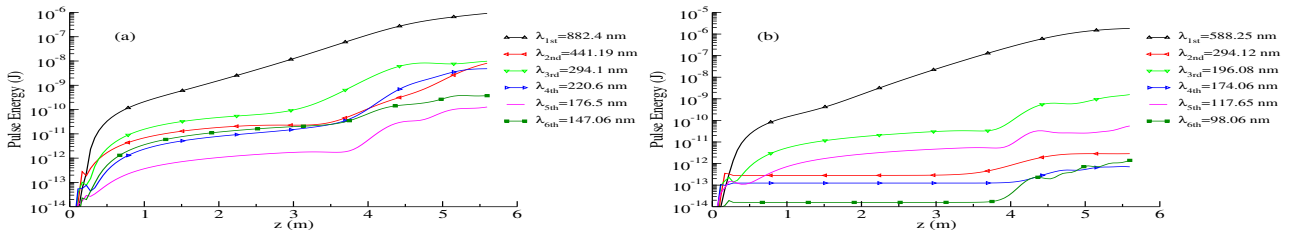


Figure 5: Evolution of pulse energy through undulator interaction for different harmonics (a) x- polarization , (b) y- polarization,  $m/n=3/2$ .

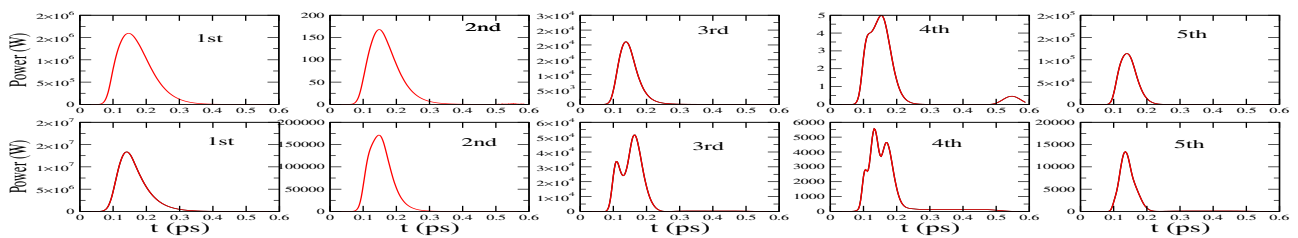


Figure 6: Power pulse shape in  $z=4.5$ , up: x-polarization, down: y-polarization;  $m/n=2$ .

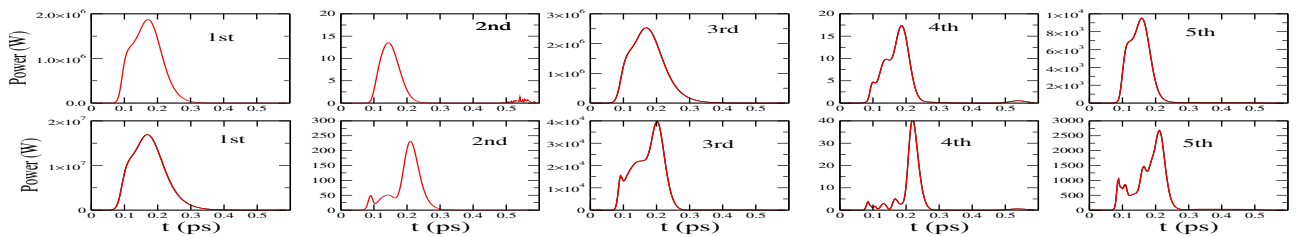


Figure 7: Power pulse shape in  $z=4.5$ , up: x-polarization, down: y-polarization;  $m/n=3$ .

## CONCLUSION

This report focuses on studying the harmonic generation in the two-orthogonal undulators in two different methods. By considering the total energy radiated per unit solid angle per unit frequency interval for a single electron traveling the undulators and also by numerical simulation of one-dimensional non-averaged equations, we have demonstrated the possibility of generation of the even and odd harmonics as well as non-integer harmonic in two orthogonal undulators.

## REFERENCES

- [1] W. Ackermann, G. Asova, V. Ayvazyan, A. Azima, and N. Baboi, *Nat. Photon.* 1, 336 (2007).
- [2] B. McNeil, *Nat. Photonics* 3, 375 (2009).
- [3] G. Dattoli, N.S. Mirian, E. DiPalma, and V. Petrillo, *Phys. Rev. ST Accel. Beams*, 17, 5, 050702, (2014).
- [4] N.S. Mirian, G. Dattoli, E. DiPalma, and V. Petrillo, *Nuclear Instruments and Methods in Physics Research Section A*, 767,227, (2014).
- [5] H.P. Freund, L. Giannessi, and W.H. Miner, Jr., *Applied Phys* 104, 123114 (2008).
- [6] N.S. Mirian, reference available at <http://particles.ipm.ir/Cyrus1D.jsp>.
- [7] N.S. Mirian, E. Salehi, reference available at <http://particles.ipm.ir/Cyrus1D.jsp>.
- [8] G. Dattoli, P.L. Ottaviani, and S. Pagnutti, Report No. ENEA RT/2007/40/FIM.
- [9] N. Mirian, B. Maraghech, *Phys. Plasmas* 21, (2014).